PROCEEDINGS OF SCIENCE

Charm current-current correlators in Twisted Mass Lattice QCD

Marcus Petschlies[*] [†]
Humboldt-Universität zu Berlin, Institut für Physik
Newtonstraße 15
12489 Berlin
E-mail: marcuspe@physik.hu-berlin.de

The $\overline{MS}$ charm quark mass is determined from moments of the charm vector current correlator in 2-flavor twisted mass lattice QCD with a heavy quark doublet in the valence sector. In a first step moments and ratios of consecutive moments are calculated which in the continuum limit can be compared directly to their experimental counterparts. By matching the nonperturbatively determined lattice moments to continuum perturbation theory the charm quark mass is extracted.

The XXVIII International Symposium on Lattice Field Theory, Lattice2010
June 14-19, 2010
Villasimius, Italy

[*]Speaker.
[†]Member of the European Twisted Mass Collaboration

 http://pos.sissa.it/

PoS(Lattice 2010)238

1. Introduction

In recent works [1, 2, 3] it has been shown that lattice QCD is a powerful tool for the determination of the charm quark mass and the strong coupling constant via the so called current-current correlator method. Precise estimates of these Standard Model parameters are one prerequisite for precision tests of QCD. We apply this method in the framework of twisted mass lattice QCD with two flavors of dynamical quarks and focus on the charm vector current correlator and charm vacuum polarization function. In continuum QCD this quantity is related by causality and unitarity to the ratio R of the hadronic cross section $\sigma(e^+e^- \to c\bar{c})$ to the leptonic one $\sigma(e^+e^- \to \nu^+\mu^-)$. In the traditional approach the charm quark mass would be extracted from moments of the ratio R using the experimental cross section data to account for the nonperturbative QCD effects in the low energy region and at flavor thresholds. Matching the perturbative expansion of the moments in terms of the strong coupling α_s and the charm quark mass $\bar{m}_c$ with their experimental values gives a defining relation for the value of the latter. A nonperturbative lattice QCD calculation of the charm contribution to the vacuum polarization function gives an alternative access to the effects of the strong interaction and hence when combined with the perturbative expansion of the latter in the $\overline{MS}$ scheme [4] allows for an R-independent determination of the charm quark mass and strong coupling constant.

2. Moments in perturbative QCD and Lattice QCD

In continuum QCD the moments of the charm contribution to the cross section ratio R are related to derivatives of the charm vacuum polarization function Π_c

$$M_n = \int \frac{ds}{s^{n+1}} R_c(s) = \frac{12\pi^2}{n!} \left(\frac{d}{dq^2}\right)^n \Pi_c(q^2)\Big|_{q^2=0} \tag{2.1}$$

where

$$\left(q_\mu q_\nu - g_{\mu\nu} q^2\right) \Pi_c(q^2) = \int dx\, \mathrm{e}^{iqx} \langle J^c_\mu(x) J^c_\nu(0)\rangle \tag{2.2}$$

and $J^c_\mu = \bar{\psi}\gamma_\mu \psi$ is the charm vector current. The perturbative expansion of the polarization function Π_c in the region where $z = q^2/(4\bar{m}_c^2) \ll 1$ has reached the 4-loop level [4].

$$\Pi_c(q^2) = \sum_{n\geq 0} \bar{C}_n z^n \tag{2.3}$$

$$\bar{C}_n = \sum_{l=0}^{3} \sum_{k=0}^{l} \bar{C}_n^{lk} \left(\frac{\alpha_s}{\pi}\right)^l \log\left(\bar{m}_c^2/\mu^2\right)^k . \tag{2.4}$$

μ denotes the renormalization scale and $\bar{m}_c = \bar{m}_c(\mu)$, $\alpha_s = \alpha_s(\mu)$ are the charm quark mass and strong coupling in the $\overline{MS}$ scheme. Given the expansion (2.3) one then has

$$M_n = \frac{12\pi^2}{(4\bar{m}_c(\mu)^2)^n} \bar{C}_n(\alpha_s, \mu) . \tag{2.5}$$

PoS(Lattice 2010)238

The dimensionless lattice moments G_m are defined in a standard way [1] via the time dependent two-point correlation function at zero spatial momentum

$$G_m = \sum_{t/a=1}^{T/(2a)-1} \left(\frac{t}{a}\right)^m (C_V(t) + C_V(T-t))$$

$$C_V(t) = Z_V^2 \frac{a^6}{3L^3} \sum_{i=1}^{3} \sum_{\vec{x}} \langle j_i^c(t,\vec{x})\, j_i^c(0) \rangle\,. \tag{2.6}$$

The renormalization factor Z_V has been determined nonperturbatively in [5]. The choice for the lattice vector current j_i^c will be given below.

To eliminate the explicit dependence on the lattice spacing the moments are multiplied by a suitable power of the light pseudoscalar decay constant $a f_{PS}$ in lattice units such that in the continuum limit and when tuned to the physical point it follows that

$$G_{2n+2}(a f_{PS})^{2n} = \left(\frac{f_\pi}{\bar{m}_c}\right)^{2n} \frac{(2n+2)!}{4^n} \bar{C}_n \quad + \text{lattice artifacts}\,. \tag{2.7}$$

$$\frac{G_{2n+2}}{G_{2n+4}(a f_{PS})^2} = \left(\frac{\bar{m}_c}{f_\pi}\right)^2 \frac{4}{(2n+4)(2n+3)} \frac{\bar{C}_n}{\bar{C}_{n+1}} \quad + \text{lattice artifacts}\,. \tag{2.8}$$

3. Lattice setup and calculation

The lattice moments G_m are estimated using the gauge field ensembles of the European Twisted Mass Collaboration [8]. In the partially quenched setup of this calculation a doublet of heavy valence quarks $\chi = (\chi_+, \chi_-)$ is added to the two dynamical light quarks in the sea sector, with $\chi_\pm$ differing by the sign of the twisted mass term as given in equation (3.1).

$$\mathscr{S}_{val} = \sum_x \bar{\chi}(x) \left(D_W + m_{0c} + i\mu_h \gamma_5 \tau^3\right) \chi(x)\,. \tag{3.1}$$

D_W denotes the massless Wilson Dirac operator, m_{0c} the critical bare mass and μ_h the bare twisted mass in the heavy quark sector.

As interpolating operators for the charm current in terms of the physical charm field Ψ^c the flavor non-singlet vector current has been used

$$j_i^c = \frac{1}{2}\left(\bar{\Psi}_+^c \gamma_i \Psi_-^c + \bar{\Psi}_-^c \gamma_i \Psi_+^c\right) = \frac{1}{2}\left(\bar{\chi}_+ i\gamma_i\gamma_5 \chi_- + \bar{\chi}_- i\gamma_i\gamma_5 \chi_+\right)$$

which corresponds to the flavor non-singlet axial vector current in the tmLQCD setup at maximal twist [9].

In the present calculation the light and heavy quark mass dependence is parameterized in terms of the dimensionless ratios $\frac{m_{PS}}{f_{PS}}$ and $\frac{m_{J/\psi}}{f_{PS}}$, respectively, which are determined from the same lattice correlator data. The physical point is then given by $\frac{m_{PS}}{f_{PS}} = 1.068(3)$, $\frac{m_{J/\psi}}{f_{PS}} = 23.69(7)$. The scale a is set via the light pseudoscalar decay constant using $f_\pi = 130.7(4)\,\mathrm{MeV}$.

Table 1 shows the data for the mass ranges the moments were calculated for. The ensembles comprise four lattice spacings and two different volumes for $\beta = 3.90$ and $\beta = 4.20$. With these sampling points the $\frac{m_{PS}}{f_{PS}}$ and $\frac{m_{J/\psi}}{f_{PS}}$ dependence of the moments and ratios is interpolated to common

β	L/a	$a\mu_l$	$a\,[\mathrm{fm}]$	$\frac{m_{PS}}{f_{PS}}$	$\frac{m_{J/\psi}}{f_{PS}}$
3.80	24	0.0060	0.0998 (19)	2.390 (20)	16.91 (10) . . . 27.59 (16)
		0.0080		2.479 (15)	15.52 (08) . . . 25.28 (12)
		0.0110		2.720 (13)	14.58 (06) . . . 23.76 (10)
		0.0165		3.042 (11)	13.39 (05) . . . 21.76 (08)
3.90	24	0.0040	0.0801 (14)	2.126 (18)	18.25 (10) . . . 31.52 (17)
		0.0064		2.426 (20)	16.69 (10) . . . 28.87 (18)
		0.0085		2.603 (19)	15.86 (09) . . . 27.38 (16)
		0.0100		2.748 (16)	15.34 (08) . . . 26.48 (13)
		0.0150		3.117 (15)	14.17 (06) . . . 24.44 (11)
3.90	32	0.0030		1.833 (14)	18.36 (10) . . . 31.75 (17)
		0.0040		2.014 (12)	17.56 (09) . . . 30.37 (15)
4.05	32	0.0030	0.0638 (10)	2.056 (23)	18.69 (14) . . . 33.65 (25)
		0.0060		2.517 (17)	16.47 (09) . . . 29.69 (16)
		0.0080		2.769 (17)	15.70 (08) . . . 28.26 (14)
		0.0120		3.126 (16)	14.48 (07) . . . 26.03 (11)
4.20	32	0.0065	0.05142 (83)	2.850 (28)	18.51 (14) . . . 31.25 (24)
4.20	48	0.0020		1.869 (20)	21.48 (15) . . . 28.98 (21)

Table 1: Mass ranges of $\frac{m_{PS}}{f_{PS}}$ and $\frac{m_{J/\psi}}{f_{PS}}$ for the present investigation. The lattice spacings were taken from [7].

reference points for all lattice spacings and the continuum limit is taken at fixed reference values of $\frac{m_{PS}}{f_{PS}}$ and $\frac{m_{J/\psi}}{f_{PS}}$. Finally, the physical point is reached by an interpolation of the continuum values in $\frac{m_{J/\psi}}{f_{PS}}$ and an extrapolation to the physical value of $\frac{m_{PS}}{f_{PS}}$.

To simultaneously model the $\left(\frac{m_{PS}}{f_{PS}}\right)^2$ and $\frac{m_{J/\psi}}{f_{PS}}$ dependence of any given specific moment or ratio $\mathscr{G}$ the ansatz in equation (3.2) is used for each lattice spacing individually to fit the sample points. The pseudoscalar decay constant in lattice units $a\,f_{PS}$ needs to be interpolated to the reference points in $\frac{m_{PS}}{f_{PS}}$ as well and here too a polynomial ansatz is employed:

$$\begin{aligned} a\,f_{PS} &= \sum_{j=0}^{N} a_j \left(\frac{m_{PS}}{f_{PS}}\right)^j \\ \mathscr{G} &= \sum_{k=0}^{M}\sum_{l=0}^{N} b_{kl} \left(\frac{m_{PS}}{f_{PS}}\right)^{2l} \left(\frac{m_{J/\psi}}{f_{PS}}\right)^k , \end{aligned} \tag{3.2}$$

where in general $M \leq 3$ and $N \leq 2$ is found to be sufficient to describe the data.

4. Results for vector moments and moment ratios

A first step of the investigation was the calculation of ratios of consecutive (even) moments of the charm vector current and the comparison to the moments derived using experimental R data [4].

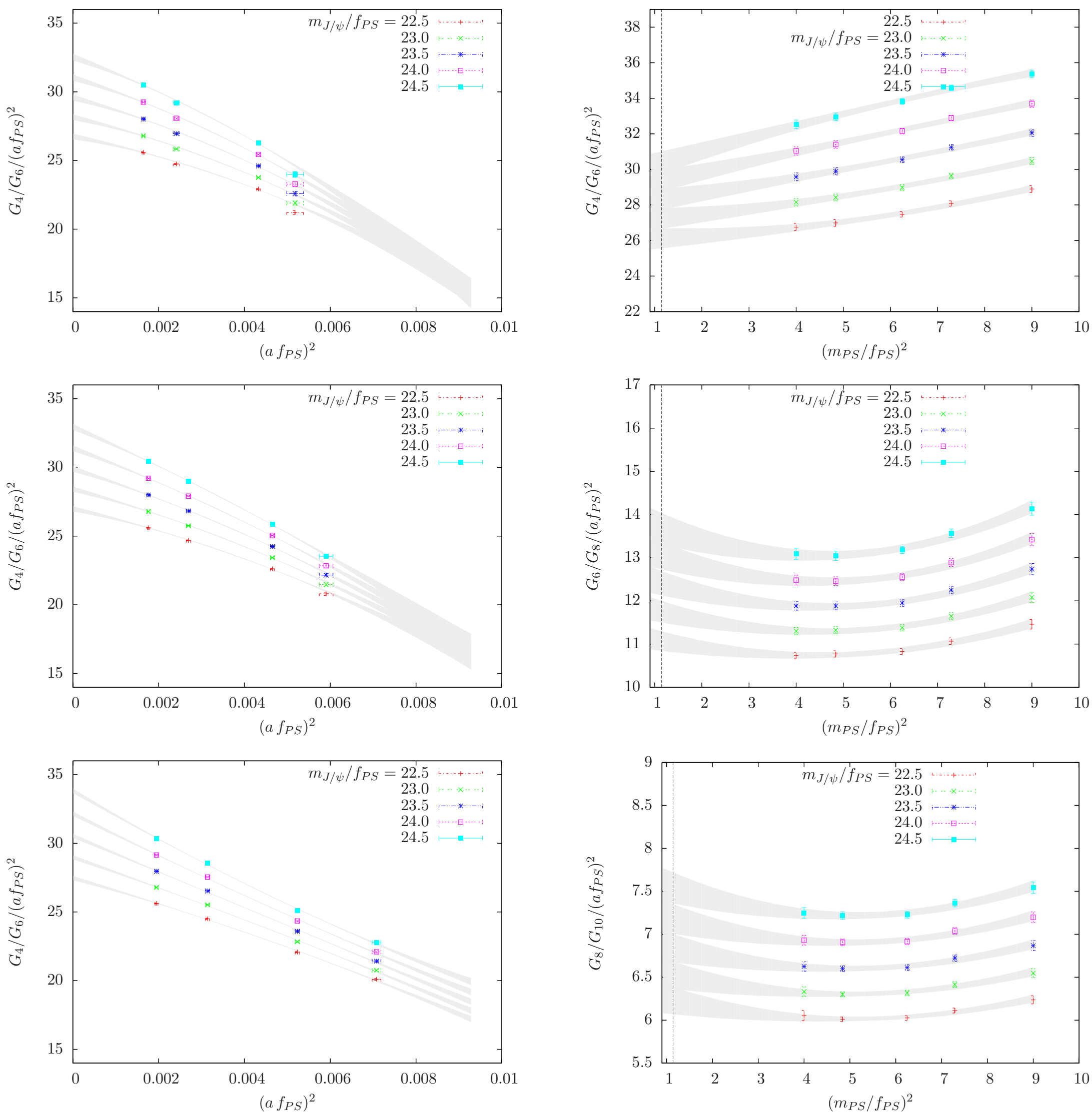

Figure 1: Examples of continuum extrapolation (left) and extrapolation in $\frac{m_{PS}}{f_{PS}}$ (right) for vector moment ratios.

As can be seen from equation (2.6) ratios of lattice moments do not require any renormalization factor (and any other normalization factors per se) and hence lend themselves to a test case.

The left panel of figure 1 shows examples of the continuum extrapolation for $G_6/G_8/(a\,f_{PS})^2$ and three fixed reference values of $\frac{m_{PS}}{f_{PS}} = 2.0, 2.2, 2.5$. Each curve in the plots represents one fixed reference value of $\frac{m_{J/\psi}}{f_{PS}} = 22.5, 23.0, 23.5, 24.0, 24.5$. Given the non-negligible curvature of the data an extrapolation ansatz taking into account a^2 as well as a^4 contributions seemed necessary. The extrapolation in $\frac{m_{PS}}{f_{PS}}$ to the physical value for G_4/G_6, G_6/G_8 and G_8/G_{10} (at fixed $\frac{m_{J/\psi}}{f_{PS}}$) is shown in the right panel of figure 1: a second order polynomial in $\left(\frac{m_{PS}}{f_{PS}}\right)^2$ seems both necessary and sufficient to describe the data. The final values at the physical point are listed in table 2; the values for the M_n are given in [4].

n	$M_{n-1}/M_n/f_\pi^2/((2n+2)(2n+1))$	$G_{2n}/G_{2n+2}/(af_{PS})^2$
2	28.23 (65)	28.72 (63)
3	11.93 (33)	12.66 (31)
4	6.83 (20)	6.97 (17)

Table 2: Comparison of continuum and lattice results for charm vector moment ratios.

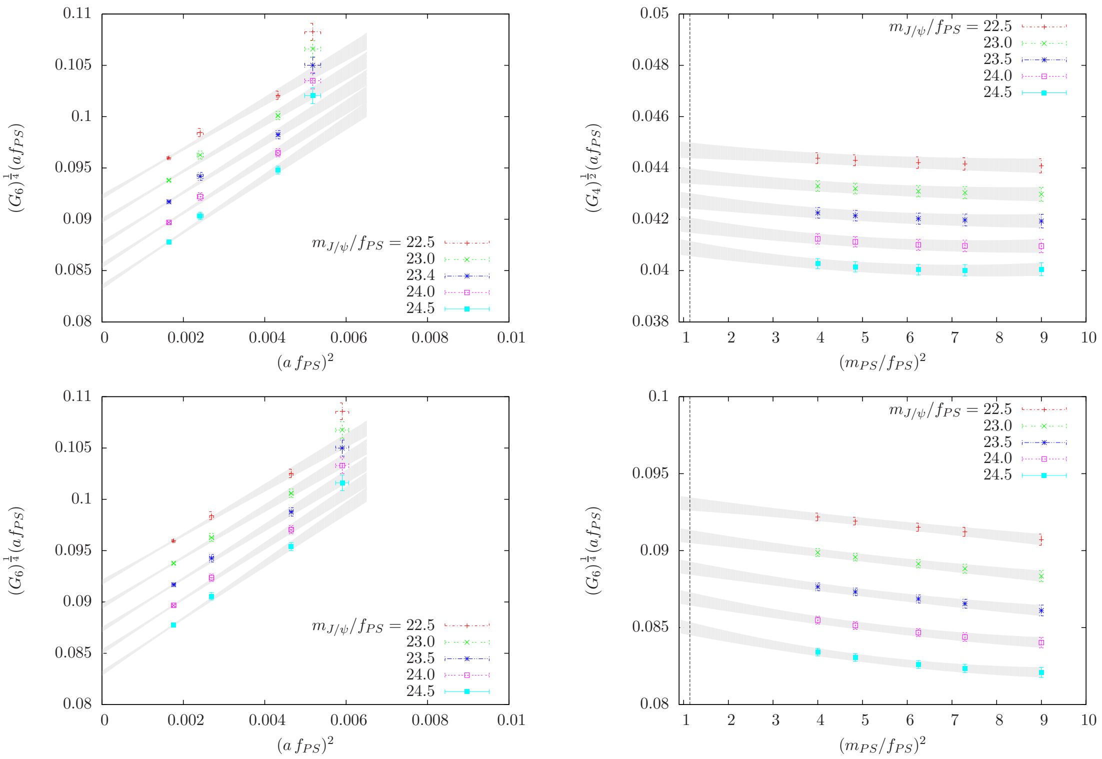

Figure 2: Examples of continuum extrapolation (left) and extrapolation in $\frac{m_{PS}}{f_{PS}}$ (right) for vector moments.

The error of the lattice result quoted in table 2 contains the statistical uncertainty from the interpolations and extrapolations and the systematic uncertainty stemming from the definition of the physical point.

Figure 2 and table 3 show analogue results for the vector moments themselves. Seeing how the data for the largest lattice spacing stands out from the remaining points the former was left out when taking the continuum limit and a linear extrapolation in a^2 was used in these cases.

The fourth column in table 3 gives the $\overline{MS}$ charm quark mass at renormalization scale $\mu = 3\,\mathrm{GeV}$ as extracted from the lattice results of the vector moments using equation (2.7). The quoted uncertainty of the quark mass contains the statistical error as well as the uncertainty of α_s. A full investigation of all systematic uncertainties is under way.

When determining the quark mass the lattice results were compared to continuum QCD with three massless and one heavy quark flavor with regard to both the input value for $\alpha_s(N_f = 4, \mu = 3\,\mathrm{GeV}) = 0.252(10)$ [1] and the definite numerical values of the coefficients $\overline{C}_n^{lk}$. This introduces

n	$M_{n-1}/M_n/f_\pi^2/((2n+2)(2n+1))$	$G_{2n}/G_{2n+2}/(af_{PS})^2$	$\bar{m}_c(\mu=3\,\mathrm{GeV})$
1	0.04107 (32)	0.04235 (33)	0.954 (13)
2	0.08792 (48)	0.08810 (52)	0.984 (15)
3	0.13081 (60)	0.13059 (68)	0.998 (15)
4	0.17106 (70)	0.17110 (82)	1.024 (10)

Table 3: Comparison of continuum and lattice results for charm vector moments together with the extracted quark mass.

a systematic error since in the present lattice calculation any effects of the strange quark as well as effects of secondary charm quark production were neglected. This systematic effect can be overcome in a future lattice calculation including dynamical strange and charm quarks [6].

5. Conclusions and outlook

The low moments of the charm vector current were calculated with results in good agreement with experimental data. Yet large lattice artifacts as well as the light quark mass extrapolation require a further careful analysis and investigation of systematic errors.

As advocated already in [1] the analysis is now being extended to include also the pseudoscalar and axial vector charm current correlators. An analysis using ETMC's $N_f = 2+1+1$ ensembles is in preparation.

6. Acknowledgements

The author is grateful for the support of the ETM Collaboration, in particular for the fruitful discussions with Karl Jansen and Carsten Urbach. This work is supported by DFG Sonderforschungsbereich/Transregio SFB/TR9-03 and DFG GK 1504.

References

[1] I. Allison *et al.* [HPQCD Collaboration], Phys. Rev. D **78** (2008) 054513 [arXiv:0805.2999 [hep-lat]].

[2] C. McNeile, C. T. H. Davies, E. Follana, K. Hornbostel and G. P. Lepage, Phys. Rev. D **82** (2010) 034512 [arXiv:1004.4285 [hep-lat]].

[3] *et al.* [HPQCD Collaboration], PoS **LATTICE2010** (2010) 231 [arXiv:1011.1208 [hep-lat]].

[4] J. H. Kuhn, M. Steinhauser and C. Sturm, Nucl. Phys. B **778** (2007) 192 [arXiv:hep-ph/0702103].

[5] M. Constantinou *et al.* [ETM Collaboration], JHEP **1008** (2010) 068. [arXiv:1004.1115 [hep-lat]].

[6] R. Baron *et al.*, JHEP **1006** (2010) 111 [arXiv:1004.5284 [hep-lat]].

[7] R. Baron *et al.* [ETM Collaboration], JHEP **1008** (2010) 097. [arXiv:0911.5061 [hep-lat]].

[8] P. Boucaud *et al.* [ETM collaboration], Comput. Phys. Commun. **179** (2008) 695 [arXiv:0803.0224 [hep-lat]].

[9] A. Shindler, Phys. Rept. **461** (2008) 37 [arXiv:0707.4093 [hep-lat]].

PoS(Lattice 2010)238